



A modified lumped parameter model of distribution transformer winding

Qingqing Ding¹, Yao Yao², Bingqian Wang³, Jingwei Fu⁴, Wei Zhang¹, Chao Zeng¹, Xiaoping Li², Stanimir Valtchev⁵



Scan for more details

1. State Key Laboratory of Power System, Department of Electrical Engineering, Tsinghua University, Haidian District, Beijing, 100084, P.R. China
2. State Grid Hubei Electric Power Co., Research Institute (HBEPRI), Hongshan District, Wuhan 430077, P.R. China
3. Flexible Transmission Engineering Department, Nari-Relays Electric Company, 210003 Nanjing, P.R. China
4. State Grid Hubei Electric Power Co., Ltd, Hongshan District, 430077 Wuhan, P.R. China
5. Department of Electrical and Computer Engineering, Faculty of Science and Technology, UNL, Portugal

Abstract: The modelling of the distribution transformer winding is the starting point and serves as important basis for the transformer characteristics analysis and the lightning pulse response prediction. A distributed parameters model can depict the winding characteristics accurately, but it requires complex calculations. Lumped parameter model requires less calculations, but its applicable frequency range is not wide. This paper studies the amplitude-frequency characteristics of the lightning wave, compares the transformer modelling methods and finally proposes a modified lumped parameter model, based on the above comparison. The proposed model minimizes the errors provoked by the lumped parameter approximation, and the hyperbolic functions of the distributed parameter model. By this modification it becomes possible to accurately describe the winding characteristics and rapidly obtain the node voltage response. The proposed model can provide theoretical and experimental support to lightning protection of the distribution transformer.

Keywords: Wide band frequency response, Distributed parameter model, Lumped parameter model, Distribution transformer, Lightning protection.

1 Introduction

Distribution transformer is an important power conversion equipment, the safe and stable operation of which ensures the reliable power supply [1]. Since the lightning induced overvoltage (LIOV), with a frequency range from power frequency to several megahertz, is the primary cause of transformer insulation fault, and the existing models are concentrated on the medium and low frequency range, it is essential to study a wider frequency band calculation model of the distribution transformer [2].

Received: 13 February, 2020/ Accepted: 23 March, 2020/ Published: 25 April 2020

✉ Qingqing Ding
ddd sunny@163.com
Yao Yao
jefferson_yao@163.com
Bingqian Wang
1037539417@qq.com
Jingwei Fu
fjw@hb.sgcc.com.cn

Wei Zhang
zhangw16@mails.tsinghua.edu.cn
Chao Zeng
zengchao_2011@163.com
Xiaoping Li
lixp@hb.sgcc.com.cn
Stanimir Valtchev
ssv@fct.unl.pt

The transformer windings modelling approaches can be roughly separated into: a) electromagnetic field modelling and b) circuit modelling. The first approach is rarely applied, as the winding structure is too complex for a numerical solution [3]. The latter one divides the transformer winding into several units, constructs the equivalent circuit of each unit and links those equivalent circuits with the electromagnetic coupling relationship between the units being considered [4]. The circuit modelling approach includes different methods of modelling: the distributed parameters model, the lumped parameter model, and the hybrid model. The last one evolves from the first two modelling methods [5].

In this paper, the amplitude-frequency characteristic of the lightning wave is analysed, and the applicable frequency ranges of different circuit models are compared. As a result, a modified wide band lumped parameter model, based on distributed parameters model, is proposed.

2 Amplitude-frequency characteristics of the lightning waveform

The lightning discharge process is very fast, and the peak current value is huge. That peak current and the overvoltage caused by it can destroy the insulation of the transformer and affect the power system reliability. The analysis of the amplitude-frequency characteristics of the lightning voltage wave is important for the realistic simulation of the lightning that strikes the transformer [6].

At present, the widely used standard waveforms of the lightning pulse voltage for experiments and simulation in international academia are the full wave shock wave [7] and the intercept wave shock wave. In the international standards like IEEE-587, BS6651, IEC62305-1, etc., the recommended lightning wave pulses for simulation and protection tests, are the following [8]:

- First lightning strike waveform: the rising time of the pulse is 10 μs and the time to half-peak is 350 μs
- Subsequent lightning strike waveform: the rising time of pulse is 0.25 μs and the time to half-peak is 100 μs
- A common test waveform: the rising time of pulses is 8 μs and the half-peak time is 20 μs

Following the Chinese Standard GB_T 7449-1987 [9], the standard waveform of the lightning shock test is defined as follows: the rising time of the pulse is 1.2 μs and the half peak time is 50 μs .

The double exponential function expression of lightning shock wave is as follows [10]:

$$u(t) = U_m (e^{-\alpha t} - e^{-\beta t}) \quad (1)$$

In (1), the U_m is the peak voltage, α and β are the wave rising slope attenuation constant and the wave tail decay

constant. According to the simplified calculation in [11], α and β have the following relations:

$$\left\{ \begin{array}{l} \alpha = \frac{1}{T_2} \ln(2U_m) \\ \beta = \frac{1}{0.6T_1} \ln\left(\frac{0.3-U_m}{0.9-U_m}\right) \end{array} \right\} \quad (2)$$

Here T_1 is the rising time of the pulses and T_2 is the half peak time. The simulated waveform of the lightning voltage, expressed in MATLAB, following the Chinese Standard GB_T 7449-1987 ($T_1 = 1.2 \mu\text{s}$, $T_2 = 50 \mu\text{s}$, $U_m \approx 1.05$) is shown in Fig.1.

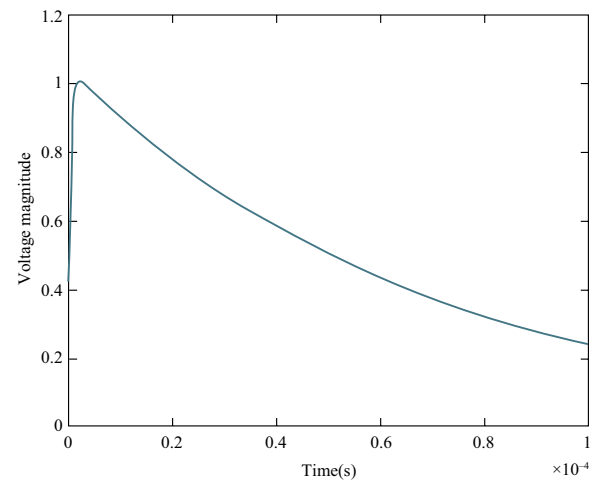


Fig. 1 Simulation of the lightning wave

The applying of the Fourier transform to the lightning shock wave expression (1) results in:

$$U(\omega) = U_m \left(\frac{1}{\alpha + j\omega} - \frac{1}{\beta + j\omega} \right) \quad (3)$$

The voltage amplitude (4) can be obtained as the module of (3):

$$|U(\omega)| = U_m \frac{\beta - \alpha}{\sqrt{(\alpha^2 + \omega^2) + (\beta^2 + \omega^2)}} \quad (4)$$

Fig. 2 and Fig. 3 show the voltage amplitude-frequency relationship for different lightning waves definitions.

According to the shown amplitude-frequency graphical relationship, it can be concluded that with the increase of the frequency, the waveform component decreases in amplitude. At a frequency of over 1 MHz, the amplitude will be very low.

Although there are several, all similar standardized lightning waveforms applied for testing, the real lightning wave that invades the transformer is not the same [12]. Its shape is far away from the standard waveform. The real

characteristics of the lightning invasion waves in substations are measured and rearranged statistically in [13]. This reference found out that there is a great difference between the actual waveform and the standard testing waveforms. As a main result, some lightning waves prove to keep high amplitude of their characteristic when the frequency is above 1 MHz. To accurately analyse the influence of the lightning wave on the distribution transformer, it is necessary to analyse the winding voltage response of the transformer in the broadband range of 0 to several terahertz and to establish a wide-band transformer model.

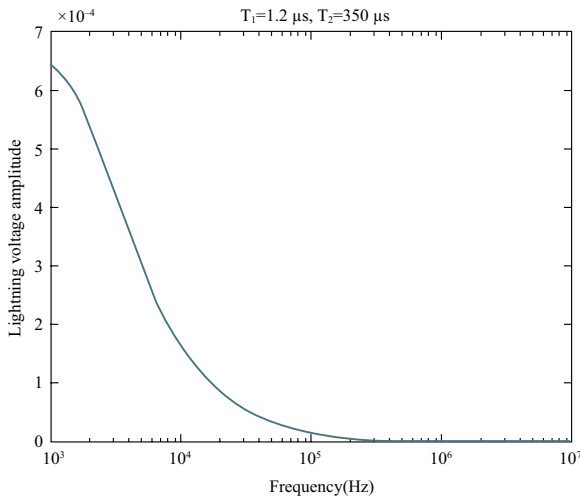


Fig. 2 Amplitude-frequency analysis of the lightning wave when $T_1 = 1.2 \mu\text{s}$, $T_2 = 50 \mu\text{s}$

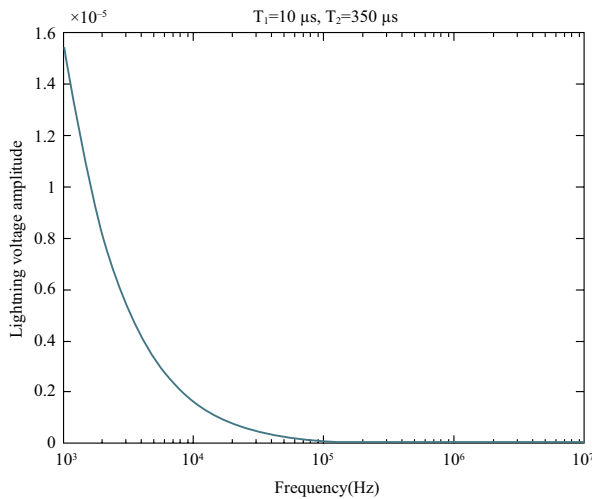


Fig. 3 Amplitude-frequency analysis of the lightning wave when $T_1 = 10 \mu\text{s}$, $T_2 = 350 \mu\text{s}$

3 Distributed and lumped parameter model of distribution transformer winding

The distributed parameter model of a transformer

winding, i.e. the multi-conductor transmission line (MTL) model, is commonly used in the large transformer winding modelling in the high frequency range [14]. This model serves to study the overvoltage response and the impedance characteristics. The lumped parameter model is generally used to analyse the medium and low frequency response (less than 1 MHz) of the transformer [15].

3.1 Distributed parameter model

The MTL model is constructed under the following assumed conditions:

- The coils of the different winding layers have the same length, which ensures the same propagation time in each transmission line and the coupling effect between the transmission lines [16, 17]. Each coil port can be treated as a node to calculate the node voltage.

- Only transverse component of electromagnetic wave (TEM) travels in the transformer winding and the radial component is ignored. The influence on the potential distribution from the bending and displacement of the windings is ignored as well [18].

In the MTL model, each coil is a unit and is treated as a straight transmission line. The voltage and current distribution in the line can be calculated by boundary conditions generated from the connecting relation of the coils [19].

The distributed parameters change with the frequency due to the nonlinearity of the iron core, the skin effect and the eddy-current effect of the conductor, which makes the frequency-domain model equations easier to be solved. The telegraph equations of the MTL model with each coil being regarded as a unit are as follows [20]:

$$\begin{cases} \frac{d\dot{U}}{dx} = -(R + sL)\dot{I} \\ \frac{d\dot{I}}{dx} = -(G + sC)\dot{U} \end{cases} \quad (5)$$

where U and I are the voltage and current vectors of each coil; the L , C , R and G are the inductance, capacitance, resistance and conductance parameter matrixes; x represents the position that begins at the head of the coils and points to their end.

Let P and T be the phase-mode conversion matrix of U and I , while $Z = R + sL$, and $Y = G + sC$, so that:

$$\begin{cases} P^{-1}ZYP = \Lambda^2 \\ T^{-1}ZYT = \Lambda^2 \end{cases} \quad (6)$$

where Λ is a diagonal matrix formed by the eigenvalues of Z and Y . The diagonal elements of Λ are the propagation constants of transmission lines. According to the equation

(5), the relation (7) can be derived:

$$P^{-1}ZT = T^{-1}YP = \Lambda \quad (7)$$

The relationships deduced in [21] between the current vector and voltage vector in the head and the end of the coils, are as follows:

$$\begin{cases} \dot{I}_s = T \coth(\Lambda)P^{-1}\dot{U}_s - T \operatorname{csch}(\Lambda)P^{-1}\dot{U}_R \\ \dot{I}_R = -T \operatorname{csch}(\Lambda)P^{-1}\dot{U}_s + T \coth(\Lambda)P^{-1}\dot{U}_R \end{cases} \quad (8)$$

Here \dot{I}_s and \dot{U}_s are the current and voltage vectors in the beginning of the coils, while \dot{I}_R and \dot{U}_R are at the end. The MTL model is equivalent to the π type circuit, shown in Fig. 4.

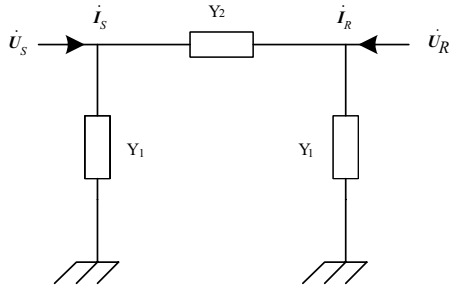


Fig. 4 A π type equivalent circuit of MTL model

The admittances are:

$$\begin{cases} Y_1 = T \tanh\left(\frac{\Lambda}{2}\right)P^{-1} \\ Y_2 = T \operatorname{csch}(\Lambda)P^{-1} \end{cases} \quad (9)$$

The MTL model can be considered equivalent to a two-terminal port, and its voltage response and input impedance can be obtained by solving the node voltage equations [22].

3.2 Lumped parameter model

The construction of the lumped parameter model of the transformer winding, is presented in Fig. 5. The elements R , L , C and G correspond to the inductance, capacitance, resistance and conductance of the longitudinal branch. Each half of C and G total value is connected at each of the two nodes respectively [23].

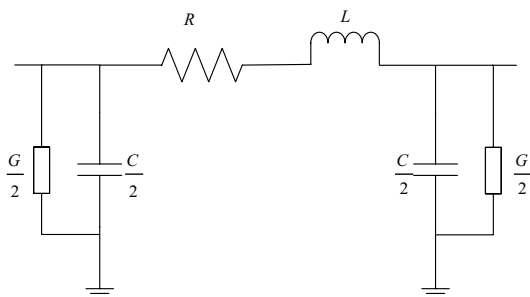


Fig. 5 The π type equivalent circuit of lumped parameter model

The lumped parameter model can be represented in the equivalent circuit of Fig. 4 and accordingly, its voltage response and input impedance can be obtained by solving the node voltage equations [24]:

$$\begin{cases} Y_1 = \frac{(G+sC)}{2} = \frac{Y}{2} \\ Y_2 = (R+sL)^{-1} = Z^{-1} \end{cases} \quad (10)$$

For the winding of the transformer, the equation can also be established, considering the head and the end of the circuit, and the voltage of the equivalent circuit.

$$\begin{cases} \dot{I}_s = \left(\frac{1}{2}(G+sC) + (R+sL)^{-1}\right)\dot{U}_s - (R+sL)^{-1}\dot{U}_R \\ \dot{I}_R = \left(\frac{1}{2}(G+sC) + (R+sL)^{-1}\right)\dot{U}_R - (R+sL)^{-1}\dot{U}_s \end{cases} \quad (11)$$

3.3 Comparison of the two π type equivalent circuits

The distributed and lumped parameter models can be compared to the π type equivalent circuit in Fig. 4. Extending the hyperbolic functions in (8), results in:

$$\begin{cases} \tanh(x) = x - \frac{1}{3}x^3 + \frac{2}{15}x^5 + \dots \\ \operatorname{csch}(x) = x^{-1} - \frac{1}{6}x^3 + \frac{7}{360}x^5 + \dots \\ \operatorname{coth}(x) = x^{-1} + \frac{1}{3}x^3 - \frac{1}{45}x^5 + \dots \end{cases} \quad (12)$$

When $|x| < \pi$, $\tanh(x) \approx x$, $\operatorname{csch}(x) \approx 1/x$. Only if the elements of Λ satisfy the condition $|j2\pi f\Lambda| \leq 1$, or if the propagation time of the electromagnetic wave through per unit length of transmission line is far less than 1, there will be another approximation done: $\tanh(\Lambda/2) \approx \Lambda/2$ and $\operatorname{csch}(\Lambda) \approx 1/\Lambda$. Under this approximation, a relation (13) exists between the parameter matrixes of the two π type equivalent circuits. Therefore, $|j2\pi f\Lambda| \leq 1$ is taken as the basis of calculating the applicable frequency range of the lumped parameter model.

$$\begin{cases} Y_1 = T \tanh\left(\frac{\Lambda}{2}\right)P^{-1} \approx \frac{1}{2}(T\Lambda P^{-1}) = \frac{1}{2}(G+sC) \\ Y_2 = T \operatorname{csch}(\Lambda)P^{-1} \approx (P\Lambda T^{-1}) = (R+sL) \end{cases} \quad (13)$$

Supposing that A_1 is the incidence matrix of nodes and coil's head, A_2 is the incidence matrix of nodes and coil's end, then the node admittance matrix is calculated:

$$Y_n = A_1 Y_1 A_1^T + A_2 Y_2 A_2^T + (A_1 - A_2) Y_2 (A_1 - A_2)^T \quad (14)$$

The node impedance matrix is the inversion of the node admittance matrix. The node input impedance and the

voltage at the node i can be obtained according to the node voltage equations:

$$Z_{in} = \frac{U_n(1)}{I_s} = Z_n(1,1) \quad (15)$$

$$U_n(i) = Z_n(i,1)I_s = \frac{Z_n(i,1)}{Z_n(1,1)}U_n(1) \quad (16)$$

4 A modified lumped parameter model

4.1 Equivalent circuit

According to Section 3, the distributed parameter model is accurate in high frequency range, and the highest applicable frequency of lumped parameter model can be defined by $|j2\pi f\Lambda| \leq 1$. The result which lumped parameter model's error occurs in several hundred kilohertz can be calculated using the parameters of common distribution transformers, and the result can be found from the following simulation.

A modified lumped parameter model is proposed in [25]. The central idea of the model is consistent with the analysis of Section 3.3, where the lumped parameter model is the low frequency approximation of a distributed parameter model. The hyperbolic functions in (12) have an approximated form as follows:

$$\left\{ \begin{array}{l} \tanh(0.5x) \approx (k_2 - k_1)x \\ \operatorname{csch}(x) \approx x^{-1} + k_1x \\ \operatorname{coth}(x) \approx x^{-1} + k_2x \end{array} \right\} \quad (17)$$

To ensure the low frequency accuracy, the model needs to meet the relation: $k_2 - k_1 = 0.5$. Thus, it needs to find the k_2 , which will minimize the sum of squares of the errors between $\operatorname{coth}(x) - x^{-1}$ and k_2x . Finally, the result is $k_2 = 0.375$, $k_1 = -0.125$.

Although the wide frequency band error decreases in lumped parameter proposed in the model, the global error cannot be guaranteed. Based on [25], this paper proposes a modified lumped parameter model, the low frequency accuracy and the global error, both get improved.

The U-I relations in (8), concerning the distributed parameter model and the U-I relations in (11), i.e. the lumped parameter model, can be combined with (7). In this case, the errors between $\operatorname{csch}(x)$ and $x^{-1} + k_1x$, and between $\operatorname{coth}(x)$ and $x^{-1} + k_2x$, decrease. The error between the two models then decreases. The absolute error between the two models is assessed by the quadratic sum of errors between hyperbolic functions and their approximated equivalent expansions in the frequency range from 0 to 5 MHz:

$$\left\{ \begin{array}{l} \operatorname{err} \operatorname{csch} = |(\operatorname{csch}(x) - (x^{-1} + k_1x))^2| \\ \operatorname{err} \operatorname{coth} = |(\operatorname{coth}(x) - (x^{-1} + k_2x))^2| \end{array} \right\} \quad (18)$$

Meanwhile, the $\tanh(0.5x) \approx 0.5x$ at low frequency, and $\tanh(0.5x) = \operatorname{coth}(x) - \operatorname{csch}(x) = (k_2 - k_1)x$. Therefore, the low frequency accuracy of the desired parameter model can be guaranteed if $(k_2 - k_1)$ is approximately equal to 0.5.

According to (12), the constraint conditions of k_1 and k_2 are as follows:

$$\left\{ \begin{array}{l} \frac{1}{3} < k_2 < \frac{1}{2} \\ k_1 < -\frac{1}{6} \\ k_2 - k_1 \approx \frac{1}{2} \end{array} \right\} \quad (19)$$

Plan (1): Without considering the constraint $k_2 - k_1 \approx 0.5$, let the derivatives of $\operatorname{err} \operatorname{csch}$ and $\operatorname{err} \operatorname{coth}$ equal to 0 to minimize them simultaneously. A pair of k_1 and k_2 is obtained: $k_2 \approx 0.3375$, $k_1 \approx -0.1703$. Therefore, (20) can be used:

$$\left\{ \begin{array}{l} \tanh(x) \approx 0.5078x \\ \operatorname{csch}(x) \approx x^{-1} - 0.1703x \\ \operatorname{coth}(x) \approx x^{-1} + 0.3375x \end{array} \right\} \quad (20)$$

Plan (2): Considering $k_2 - k_1 = 0.5$ to guarantee the low frequency accuracy, let the partial differential of sum of $\operatorname{err} \operatorname{csch}$ and $\operatorname{err} \operatorname{coth}$ equal to 0. A pair of k_1 and k_2 is obtained: $k_2 \approx 0.3336$, $k_1 \approx -0.1664$. Therefore:

$$\left\{ \begin{array}{l} \tanh(x) \approx 0.5x \\ \operatorname{csch}(x) \approx x^{-1} - 0.1664x \\ \operatorname{coth}(x) \approx x^{-1} + 0.3336x \end{array} \right\} \quad (21)$$

Comparing the hyperbolic approximated functions shown in (20), (21) and (17), the errors between lumped parameter models and distributed parameter model can be depicted in Fig. 6 and Fig. 7.

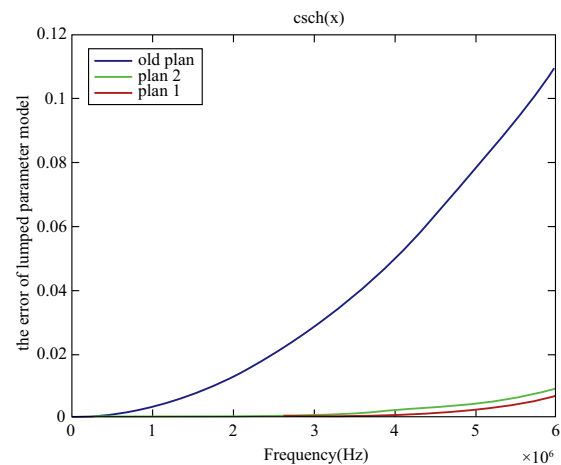


Fig. 6 Relative error of the equivalent equation of $\operatorname{csch}(x)$

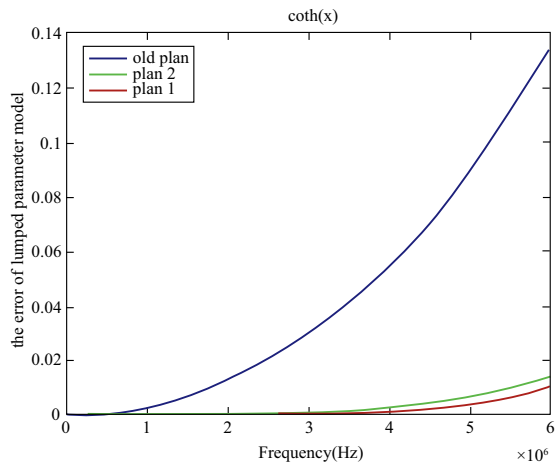


Fig. 7 Relative error of the equivalent equation of $\coth(x)$

According to Fig. 6 and Fig. 7, the applicable frequency ranges of the values of k_1 and k_2 in plan (1) and plan (2) are 0~5 MHz, both wider than the traditional lumped parameter model. The plan (1) has a smaller global error and the plan (2) has a better low frequency accuracy. Considering that the plan (1) has much smaller high frequency error and its low frequency error is also within the allowed error range, k_1 and k_2 in plan (1) are chosen as the simulation parameters. In this case the Y_1 and Y_2 of the modified lumped parameter model are as follows:

$$\begin{cases} Y_1 = 0.5078(G + sC) \\ Y_2 = (R + sL)^{-1} - 0.1703(G + sC) \end{cases} \quad (22)$$

In the lumped parameter model with a line turn as a unit, the equivalent circuit of the unit line turns is shown in Fig. 8.

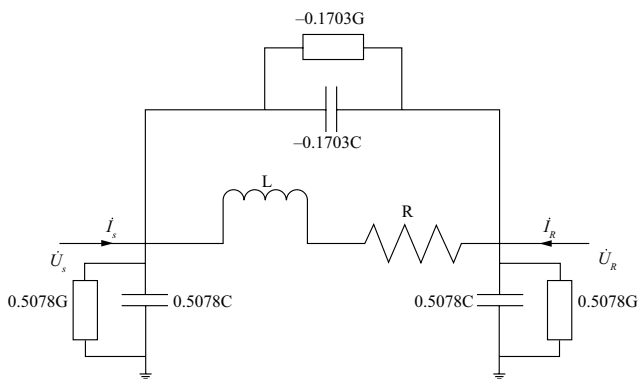


Fig. 8 Lumped parameter model equivalent circuit

4.2 Modelling and simulation

The chosen transformer is a S9 series, 100 kVA, three phase 50 Hz, 10/0.4 kV, oil-immersed natural convection cooled transformer. To simplify the computation of the simulated object, only one phase of the winding with technical parameters, as in Table 1, is considered.

Table 1 Technical parameters of transformer core and coil

Coil Diameter	High-Voltage Coil		Low-Voltage Coil	
	Wire	Turns	Wire	Turns
135 mm	Φ1.7 mm	1260	4×9 mm	52

To calculate the interturn capacitance, interlayer capacitance and ground capacitance and to form the capacitance parameter matrix C , the plate capacitance method and the coaxial cylinder method from [26] are used. The parameters L and G are calculated from their relationship with C . The R can be calculated from empirically fit formulas.

Uniformly sampling 500 frequency points from 0 to 5 MHz range, a simulation and calculation of the node voltage response of the transformer winding according to the MTL model, is done. The original lumped parameter model and the modified lumped parameter model, respectively, are applied in the calculations. The amplitude-frequency characteristics of the voltage transfer function at the node at No. 217, or the head-end of the 9th coil of the 7th layer, are depicted as in Fig. 9.

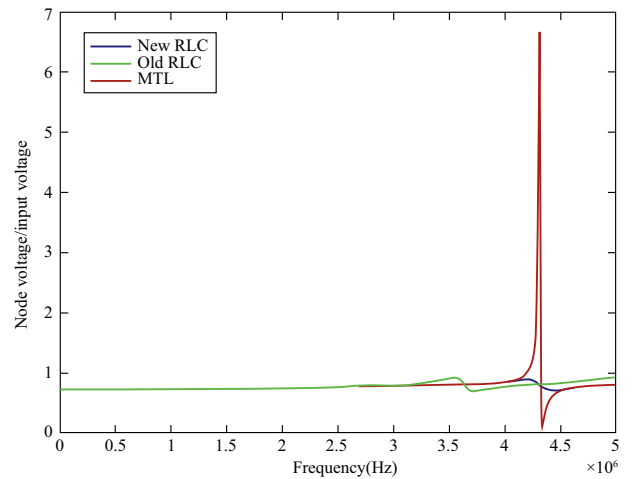


Fig. 9 Amplitude-frequency characteristic of voltage transfer function at No. 217 node

The characteristic in Fig. 9 shows that the simulation results of the original Lumped parameter model and the MTL model differ significantly when the frequency is higher than 2 MHz. The results of the proposed modified lumped parameter model and the MTL model almost coincide with each other from 0 to 5 MHz, which proves that the applicable frequency range is extended by the proposed model to about 5 MHz.

The physical significance of the modified model is proved by the capacitance and admittance behaviour in

parallel with the longitudinal inductance. As an example, a lossless transmission line is taken. It has been mentioned above that the propagation time of a unit length transmission line should be much lower than 1, i.e. $|j2\pi f\Lambda| \leq 1$, or the coil parameters have to satisfy the condition $\sqrt{\omega C} \leq 1/\sqrt{\omega L}$. This means that the node admittance to the earth is much lower than the internode admittance [27]. The coil parameters will meet the above conditions when frequency is low enough and will no longer meet the condition when the increasing frequency results in the increase of the node admittance to the ground and the decrease of the internode admittance. That latter case makes the energy consuming at the inductance branch to increase and the voltage wave is no longer propagated along the coil from the head to the end, so that the error in the lumped parameter circuit occurs.

The internode admittance being an admittance branch in parallel with the inductance branch, as in Fig. 8, will not decrease all the way with the increase of the frequency. The susceptance of the parallel capacitor branch increases with the frequency, which is helpful for the propagation of energy from the head to the end of the coil. Hence, the modified lumped parameter model equals to an adding of a compensating capacitor to the longitudinal inductor branch.

5 Conclusion

This paper proves that the lumped parameter model and the MTL model can be equivalent to a π type circuit. After analysing the similarities and differences between these two models, a modified lumped parameter model is proposed. In conclusion, the simulation results from the proposed model, verify that the applicable frequency range of the lumped parameter model is extended up to 5 MHz. This result provides a theoretical basis, capable to enlarge the research to an important experimental knowledge, ensuring that the future power system will be more predictable and hence, more reliable. The further research on the protection of the distribution transformer windings insulation will continue, making less the cost of the protection and safer the exploiting and the repairment.

Acknowledgements

This work was supported by the National Key Research and Development Plan of China under Grant (2016YFB0900600XXX).

References

- [1] Xu P, Li S, Gan P, et al (2011). Analysis of Lightning-strike Fault of Distribution Transformer and Study on Lightning Protection Measures. Insulators and Surge Arresters, Vol.4, pp: 61-66
- [2] Gustavsen B (2004) Wide band modeling of power transformers. IEEE Transactions on Power Delivery, 19(1): 414-422
- [3] Liang G, Sun H, Zhang X, et al (2006) Modeling of transformer windings under very fast transient overvoltages. IEEE Transactions on Electromagnetic Compatibility, Vol. 48, pp: 621-627
- [4] Mombello EE, Zini HC (2007) A novel linear equivalent circuit of a transformer winding considering the frequency-dependence of the impedances. Electric Power Systems Research, 77(8): 885-895
- [5] Liu Q, Zhang Y, Cheng Y (2008) Research on Protection Against Lightning Over-voltage on Transformer in a 220 kV GIS Substation. High Voltage Apparatus, 44(4): 329-331
- [6] Fu M, Tang L, Peng L (2008). Study on the Lightning Protection Problem of Distribution Transformer. Insulators and Surge Arresters, 39(5): 34-37
- [7] Alexandru BM, Mihai MP, Marian C, et al (2014) Calculation methods for lightning impulse voltage distribution in power transformers. In: International Conference on Optimization of Electrical & Electronic Equipment, IEEE
- [8] Shi S (2015) Applied Research on the Port Model of Transformer Windings Based on Transmission Line Theory. (Master dissertation, North China Electric Power University)
- [9] GB_T 7449-1987, Guide to the lightning impulse and switching impulse testing of power transformers and reactors
- [10] Chen S, Wang X, Li B, et al (2006) Frequency Spectrum of Standard Lightning Currents and Its Application. Meteorological Monthly, 32(10): 11-19
- [11] Liang X, Zhou Y, Zeng R (2003) High Voltage Engineering. Tsinghua University Press
- [12] Suwanasri T, Homklinkaew S, Suwanasri C (2009) Effects of lightning impulse on power transformer insulation level. Electrical Engineering/Electronics, Computer, Telecommunications and Information Technology, 2009. In: ECTI-CON 2009. 6th International Conference on. IEEE
- [13] Sima W, Lan X, Yang Q, et al (2015) Statistical Properties and Test Analysis of the Measured Lightning Invasion Waves in a Substation. High Voltage Engineering, 41(1): 21-27
- [14] Zhao C, Ruan J, Du Z, et al (2009) Calculation of parameters in transformer winding based on the model of multi-conductor transmission line. High Voltage Apparatus, 45(04): 41-46
- [15] Chen W, Hu J, Wang Y (2006) Hybrid lumped parameter transformer winding model for very fast transient. Journal of Chongqing University, 029(009): 38-43
- [16] Yang Y, Wang Z (2009) Wide band modeling of large power transformer windings for very fast transient overvoltage (VFTO) analysis. Sci China Ser E-Tech Sci, 52(9), 2597-2604
- [17] Bakhsh FI, Irshad M, Asghar MSJ (2011) Modeling and simulation of variable frequency transformer for power transfer in-between power system networks. In: India International Conference on Power Electronics, IEEE
- [18] Mitchell SD, Welsh JS (2011) Modeling power transformers to support the interpretation of frequency-response analysis. IEEE Transactions on Power Delivery, 26(4): 2705-2717

- [19] Abed NY, Mohammed OA (2010) Physics-based high-frequency transformer modeling by finite elements. *IEEE Transactions on Magnetics*, 46(8): 3249-3252
- [20] Meng C, Li Y, Jie J, et al (2013) Calculation and Analysis of Inductance Parameters of Transformer Equivalent Circuit under Lightning. *Transformer*, 050(004): 28-32
- [21] Y. Yang, Z.-J. Wang, X. Cai, & Z.D. Wang. (2011). Improved lumped parameter model for transformer fast transient simulations. *Electric Power Applications Iet*, 5(6), 479-485
- [22] Ruan L, Zhao C, Ruan J, et al (2009) Calculation of Distributed Parameters of Transformer Winding Based on the Model of Multi-conductor Transmission Line. *High Voltage Apparatus*, 4, 011
- [23] Tran-Anh T, Auriol P, Tran-Quoc, T(2006, October). High frequency power transformer modeling for power line communication applications. In: *Power Systems Conference and Exposition, 2006. PSCE'06. 2006 IEEE PES* (pp. 1069-1074), IEEE
- [24] Popov M, van der Sluis L, Paap GC, et al (2002) Computation of very fast transient overvoltages in transformer windings. *Power Engineering Review IEEE*, 22(10), 62-62
- [25] Yu Y (2009) Study on the Modeling of Large Power Transformer Windings for Very Fast Transient Simulations. (Doctoral dissertation, Tsinghua University)
- [26] Tang M (2012) Analysis of the transient overvoltage caused by the lightning pulse in the transformer winding. ((Master dissertation, Huazhong University of Science and Technology)
- [27] Rahimpour E, Christian J, Feser K, et al (2002) Transfer function method to diagnose axial displacement and radial deformation of transformer windings. *Power Delivery, IEEE Power Engineering Review* 22(8):70 - 70

Biographies



Qingqing Ding received her bachelor and master degrees in Electrical Engineering from Tsinghua University, Beijing, China. Now, she is an associate professor of Department of Electrical Engineering in Tsinghua University. Her major fields of interests include Nonlinear Control of Power System, System Measurement and Control Technology and Lightning Protection.



Yao Yao received Ph.D. degree at Wuhan University, Wuhan, 2008. He is working in State Grid Hubei Electric Power Co. Research Institute (HBEPRI), Wuhan. His research interests include high voltage and insulation technology, power system overvoltage and insulation co-ordination, transmission line disaster prevention and reduction.



Bingqian Wang received her bachelor degree in Electrical Engineering from Huazhong University of Science and Technology, Wuhan, China, in 2014. She received her master degree in Electrical Engineering from Tsinghua University, Beijing, China, in 2017. Now, she is working at Nari-Relays electric Co., Ltd., Nanjing, China. Her major fields of interest are Lightning Protection and HVDC Control and Protection.



Jingwei Fu received master degree at Northeast Electric Power University, Jilin, 1986. He is working in State Grid Hubei Electric Power Co., LTD., Wuhan. His research interests include electric power market, development planning and Marketing.



Wei Zhang received his bachelor degree in Electrical Engineering in 2016 and is working towards his master degree at Tsinghua University, Beijing, China. His research interest includes transformer modelling and lightning protection.



Chao Zeng received his bachelor degree in Electrical Engineering from Huazhong University of Science and Technology, Wuhan, China, in 2015. He is currently pursuing his master degree in Tsinghua University, Beijing, China. His research interests include lightning induced overvoltage calculate and UAV.



Xiaoping Li received master degree at Huazhong University of Science and Technology, Wuhan, 1995. He is working in State Grid Hubei Electric Power Co. Research Institute (HBEPRI), Wuhan. His research interests include power system analysis and power quality.



Stanimir Valtchev (IEEE Senior Member'08) best graduate of 1974, Technical University Sofia (TUS), in semiconductor and electronics technology, Auxiliary Director of Centre of Robotics of TUS, 1987 assistant professor in TU Delft/NL and in TU Sofia/Bulgaria (Power Supplies and Converters), vice dean of foreign students of TUS. Now in UNL/Portugal, Invited Full Professor of Burgas Free University, and Invited Professor of TUS, Bulgaria. On advisory Board in Skoltech/Moscow and BJTU/Beijing, General Chair of the IEEE-PEMC2016 conference and Chair of Subcommittee in IES of IEEE.

(Editor **Chenyang Liu**)